Journal of Materials Chemistry A

Accepted Manuscript

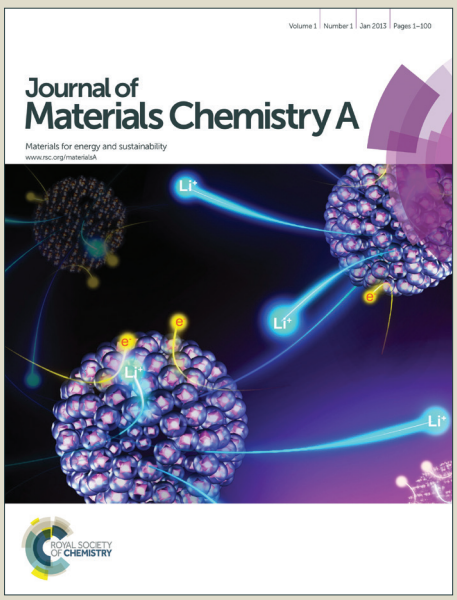

ROYAL SOCIETY OF CHEMISTRY

www.rsc.org/materialsA

Journal of Materials Chemistry

Cite this: DOI: 10.1039/c0xx00000x

www.rsc.org/xxxxxx

ARTICLE TYPE

The effects of Au species and surfactant of Au@SiO_2 on catalytic reduction of 4-nitrophenol

Zhihua Wang, Huifen Fu, Dongmei Han, Fubo Gu*

Received (in XXX, XXX) Xth XXXXXXXXX 20XX, Accepted Xth XXXXXXXXX 20XX

DOI: 10.1039/b000000x

Au-based nanocatalysts are usually capped with surfactant and cannot be directly used. Thermal annealing is an effective method for surface cleaning. However, the effect of Au species on activity in thermal annealing process is always ignored. We studied the effects of surfactant and Au species on catalytic performance using Au@porous SiO_2 (Au@pSiO_2). It was found that the Au@pSiO_2 annealed at different temperatures showed different performances toward the reduction of 4-nitrophenol at the same time when the size of Au was maintained. The activity of the annealed Au@pSiO_2 was higher than that of the untreated sample. The sample annealed at 500 ^oC had the best performance and the catalytic activity was higher than that of the Au-based catalysts reported in the literatures. It was concluded that cationic Au species and the surfactant PVP had a combined effect on catalytic performance. The removal of the surfactant PVP from the surfaces of the Au NPs during thermal annealing process enhanced the activity, and the cationic Au species played a vital role in catalytic performance. The results are beneficial to surface cleaning and pretreatment condition determining. Surprisingly, there was an induction period for the untreated Au@pSiO_2 in the catalytic process because PVP blocked the adsorption and migration of 4-nitrophenol on the surface of the Au. The disappearing of the induction period for the annealed samples can be attributed to the removal of PVP.

Introduction

Au nanoparticles (NPs) have made great progress because of excellent properties and outstanding activities in many fields.[1-4] Au NPs supported and alone are usually surrounded by surfactants and cannot be directly used as catalysts.[5-7] Au-based catalysts are usually annealed at high temperatures to remove surface impurities. However, in the thermal annealing process, the effect of Au species on catalytic activity is always ignored.

Surfactants on nanoparticle surface block active sites and impact the catalytic activity negatively.[8,9] Thermal annealing is an effective method for surface cleaning. Li's group[10] utilized three methods to remove surfactant on Pt NPs and studied the effect of the surfactant removal on the electrocatalytic performance. The results showed that low-temperature thermal annealing (~185 ^oC) in air was found to be the most effective for surface cleaning without inducing changes of particle size and morphology. However, the changing of the nature of the Pt NPs, which was significant in catalysis, was ignored during the thermal annealing process.

For Au NPs, the activities strongly depend upon their sizes and Au species. The effect of Au species on catalyst is still being debated. Cationic Au species have been found to be more important than metallic state Au species for oxidation reactions.[11-13] However, little attention has been paid to the effect of Au species on catalytic activity in reduction reactions.[14] In fact, it is difficult to investigate the effects of Au species on catalytic performance because the synthesized structure of NPs supported and alone both deform and are different from those of pristine NPs at high temperatures. Therefore, data and results obtained from those deformed NPs are inaccurate. Au species affect the catalytic activity greatly, so understanding the effect of Au species on performance at the same time when the size of Au is maintained is urgent.

Core-shell NPs can effectively protect noble metal NPs from aggregation. To satisfy the requirements of different application fields, a series of core-shell NPs were synthesized, such as Au@Cu_2O,[15-17] Au@TiO_2,[18,19] Pd@CeO_2[20] and Au@Fe_3O_4.[21,22] As a material of shell, amorphous SiO_2 has been studied extensively due to its high thermal stability, biocompatibility and functionalization.[23,24] SiO_2 shell is inert and provides convenience for exploring the effects of Au species and surfactant on catalytic performance.

Herein, Au@porous SiO_2 (Au@pSiO_2) nanocatalysts were synthesized by using typical Stober method combined with hydrothermal etching. Thermal annealing in air was used to change surface properties of Au at the same time when the size of the Au was maintained. We carried out the reduction of 4-nitrophenol (4-NP) with $NaBH_4$ reaction to explore activities of the Au@pSiO_2 (Scheme 1). The activity of the annealed Au@pSiO_2 was higher than that of untreated Au@pSiO_2. The Au@pSiO_2 annealed at different temperatures showed different performances and the samples annealed at 500 ^oC had the best

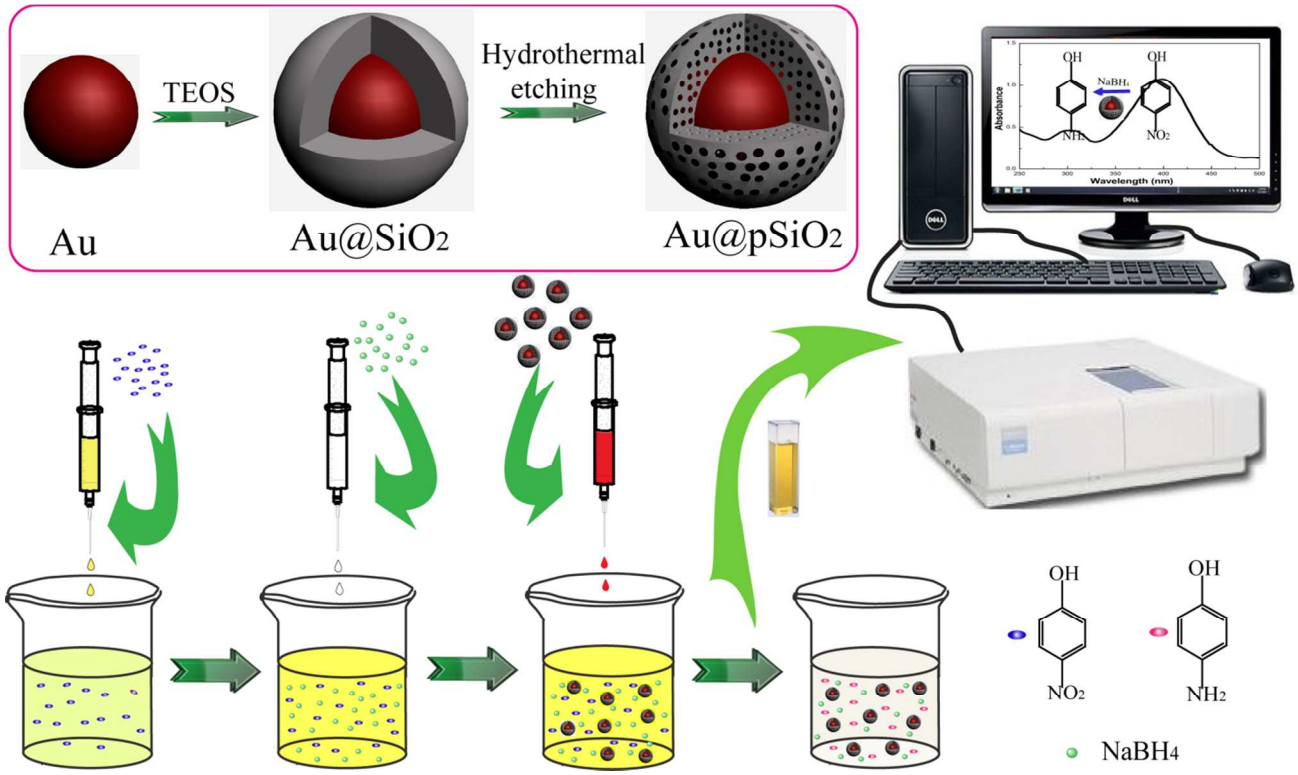

Scheme 1 Schematic illustration of the experimental procedure. Left top: synthetic route of Au@pSiO$_2$. Down: catalytic procedure of the reduction of 4-NP over Au@pSiO$_2$.

performance. It was concluded that cationic Au species and the surfactant PVP had a combined effect on catalytic performance. The removal of the surfactant PVP from the surfaces of the Au NPs during thermal annealing process enhanced the activity, and the cationic Au species played a vital role in catalytic performance. Furthermore, induction period was found in the process of the reduction reaction. For untreated Au@pSiO$_2$, the surfactant PVP on the surfaces of the Au NPs hindered the diffusion and migration of 4-NP, resulting in the emerging of the induction period. The removal of PVP from the surfaces of the Au NPs for the annealed Au@pSiO$_2$ led to the disappearing of the induction period. The removal of the surfactant is necessary to obtain high-activity catalysts, and the annealing temperature should be appropriate because of the changes of Au species.

Experimental

Materials. Chloroauric acid (HAuCl$_4$•3H$_2$O) was purchased from Sinopharm (Shanghai, China). Ammonium hydroxide (NH$_3$•H$_2$O, 25 % by weight in water) and sodium citrate were purchased from Beijing Chemical Works (Beijing, China). Poly(vinyl pyrrolidone) (PVP K30) was purchased from Beijing Yili Fine Chemical Research Institute (Beijing, China). Tetraethylorthosilicate (TEOS) was purchased from Xilong Chemical Co., Ltd. (Guangdong, China). All chemicals were analytical-grade reagents and used as received without further purification.

Preparation of Au@pSiO$_2$ NPs. Au NPs were prepared according to a previously reported method with slight modification.[25] In a typical synthesis, 4.5 mL HAuCl$_4$ • 3H$_2$O (4 g/L) and 30 mL deionized water were added in a three-neck flake, and then put in an oil bath. The oil bath was heated to 150 ^{o}C and kept for 30 min under vigorous stirring. A condenser was fixed on the three-neck flake to keep the constant of the solution volume. 1.0 mL sodium citrate aqueous solution (3.0 wt %) was injected quickly into above-mentioned solution and then refluxed for 30 min. After the solution was cooled down to room temperature, an aqueous solution of PVP K30 (0.03 g/mL, 0.65 mL) was added to the colloidal Au solution in order to modify the surfaces of AuNPs to facilitate silica coating. The solution was stirred for 12 h at room temperature. PVP-modified Au were collected by centrifugation (9000 rpm, 30 min) and redispersed in 10 mL water under ultrasonic wave. 5.0 mL PVP-modified Au was added to 18 mL ethanol and vibrated for 2 min in an oscillator. A solution of TEOS (0.1 mL) in ethanol (2.0 mL) was injected into the above solution under vigorous stirring. Then, 0.65 mL NH$_3$•H$_2$O was added to the above solution. The reaction mixture was stirred for 1 h. Then a half of the solution was added to a 100 mL Teflon-lined stainless autoclave containing 30 mL water. The Teflon-lined stainless autoclave was transferred into an oven, heated at 393 K for 30 min and cooled to room temperature. The synthesis route to Au@pSiO$_2$ nanoparticles is illustrated in Scheme 1. (a) the synthesis of monodispersed Au; (b) coating a dense SiO$_2$ shell on the surface of the Au by hydrolytic condensation of TEOS; (c) the converting of the dense SiO$_2$ shell into the mesostructure by using hydrothermal etching. The products were centrifuged (9000 rpm, 30 min) and washed with ethanol. Finally, the products were dried at 60 ^{o}C and then heated from room temperature to 350 ^{o}C, 500 ^{o}C and 700 ^{o}C with a

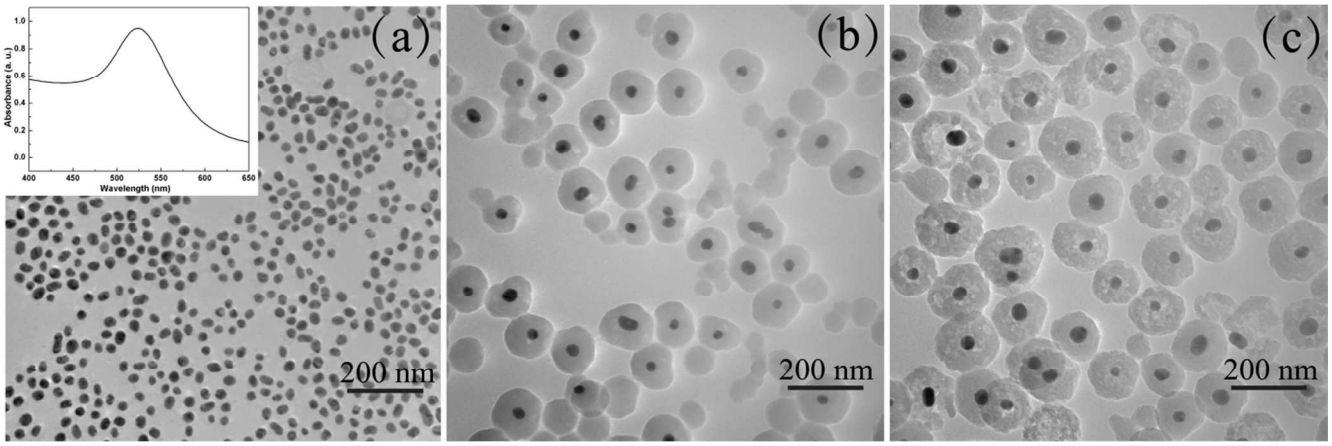

Fig. 1 TEM images of (a) Au NPs, (b) Au@dense SiO_2, and (c) Au@porous SiO_2. The inset shows the UV-Vis spectrum of the Au NPs.

heating rate of 5 °C/min and annealed at 350 °C, 500 °C and 700 °C each for 2 h.

Preparation of Au/SiO_2 NPs. 10.0 mL water was added to 36 mL ethanol at 30 °C. 2 min later, a solution of TEOS (0.2 mL) in ethanol (4.0 mL) was injected under vigorous stirring. Then, 1.30 mL NH_3•H_2O was added to the above solution. The mixture was stirred for 1 h. The product was centrifuged and dispersed in 36 mL ethanol by using ultrasonic wave. The PVP-modified Au was added to the solution. After 1 h, the product was centrifuged and washed with ethanol. Finally, the products were dried at 60 °C and then heated from room temperature to 350 °C, 500 °C and 700 °C with a heating rate of 5 °C/min and annealed at 350 °C, 500 °C and 700 °C each for 2 h. The SiO_2-supported Au (Au/SiO_2) was obtained.

Characterization. The morphologies of the samples were characterized by using transmission electron microscopies (TEM, Hitachi-800 and JEM-3010). TEM samples were prepared by dropping the NP solution onto a carbon coated copper grid. FTIR spectra were recorded from 500 cm^{-1} to 4000 cm^{-1} at room temperature by using a 370MCT IR spectrophotometer. UV-Vis spectra were recorded from 250 nm to 600 nm at room temperature by using a UV-3010 UV-Vis spectrophotometer. The X-ray diffraction (XRD) patterns of the samples were conducted on a D/Max2500V diffractometer with Cu Kα radiation by using Au@pSiO_2 powder. Thermo gravimetric analysis (TGA) was conducted in air by using a TA Instruments Q500, and the heating rate was set to 10 °C/min. X-ray photoelectron spectra (XPS) were carried out on a VG Scientific ESCALAB 250 spectrometer. Au@pSiO_2 NPs were ground in an agate mortar for 10 min before preparing the XPS samples.

Catalytic reduction of 4-nitrophenol. The reduction of 4-nitrophenol (4-NP) to 4-aminophenol (4-AP) by $NaBH_4$ was chosen as a model reaction for testing and comparing the efficiencies of different catalysts. Typically, 2 mL of 1 mM 4-NP aqueous solution was added to 16 mL deionized water and then mixed with 2 mL of 100 mM $NaBH_4$ aqueous solution. The mixture was stirred to form a uniform solution, and then 0.1 mg catalyst (Au@pSiO_2, Au wt: 26.77 %) was added. After introducing the catalyst, the bright yellow solution gradually faded as the reaction progressed. The UV-Vis spectra of the solution were recorded every 2 min during the course of the reaction (Scheme1).

Catalytic reduction of 4-NP over Au@pSiO_2 activated by $NaBH_4$ or 4-NP beforehand. Typically, an amount of catalyst (0.1 g/mL untreated Au@pSiO_2) was added to the mixture of 16 mL deionized water and 2 mL of 100 mM $NaBH_4$ aqueous solution (or 2 mL of 1 mM 4-NP aqueous solution), and stirred (or activated) for 15 min. Then, 2 mL of 1 mM 4-NP aqueous solution (or 2 mL of 100 mM $NaBH_4$ aqueous solution) was added in to trigger the catalytic reaction. The UV-Vis spectra of the finally obtained solution were recorded during the course of the reaction every 2 min. For comparison, a catalytic reaction without the activation process was also carried out.

Results and discussion

Synthesis and Characterization of Au@pSiO_2 NPs. The Au@pSiO_2 was synthesized by typical Stober method combined

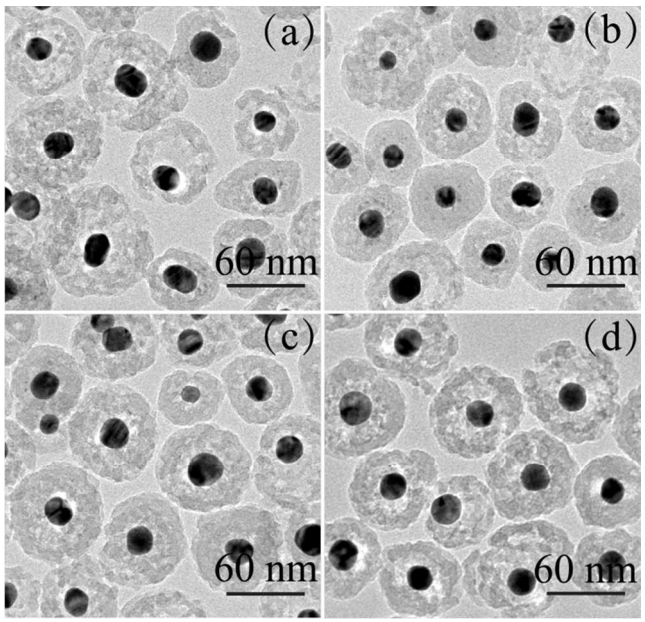

Fig. 2 TEM images of Au@pSiO_2 annealed at different temperatures: (a) without annealing, (b) 350 °C, (c)500 °C, and (d)700 °C

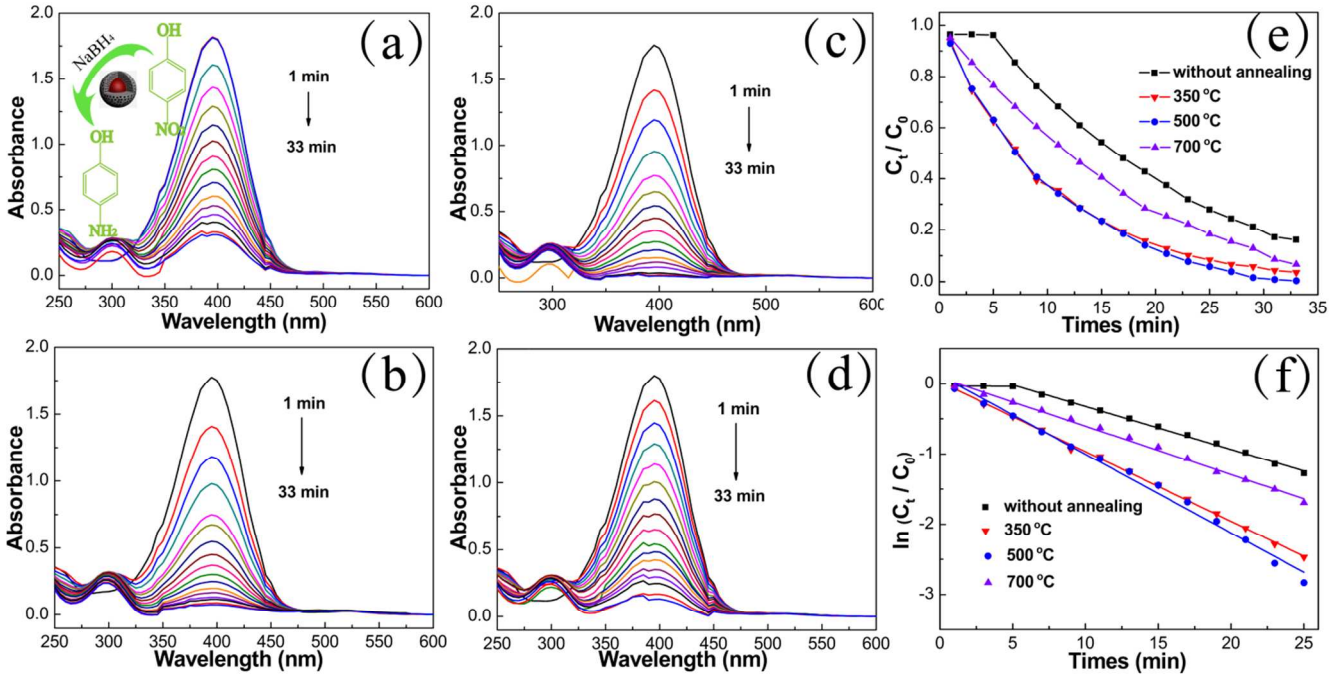

Fig. 3 Time-dependent UV-Vis spectra for the reduction of 4-NP with the Au@pSiO$_2$ annealed at different temperatures: (a) without annealing, (b) 350 °C, (c) 500 °C, (d) 700 °C, (e) time-dependent conversion curves, and (f) plot of ln(C_t/C_0) against reaction time for the four samples.

with hydrothermal etching in the presence of the dispersed Au. It is observed that the Au NPs with an average size of 30 nm are dispersed well. The peak centered at 523 nm is the typical characteristic of the Au NPs in UV-Vis spectrum shown in the inset of Fig. 1a. As can be seen from Figs. 1b and 1c, the size of the Au NPs is 30 nm in the Au@pSiO$_2$, which is similar to that of the dispersed Au NPs, and the average diameter of the Au@pSiO$_2$ is about 100 nm. SiO$_2$ shells uniformly encapsulate the Au, and the Au cores show a darker contrast than the SiO$_2$ shells. The Dense SiO$_2$ shells are converted into a porous structure after hydrothermal etching, and the surface of the Au@pSiO$_2$ are rougher than those of Au@SiO$_2$ because of the etching during hydrothermal process.

It was reported that SiO$_2$ formed by using a typical Stober method was inhomogeneous in nature. The outer layer of the SiO$_2$ was more chemically robust than the inner layer, which can be selectively etched by hot water.[26] Therefore, the etching process started from the inner layer of the SiO$_2$, forming the porous structure finally. In this work, during the hydrothermal process, hot water can attack the generated SiO$_2$ from the softer inner section when excess water was added to break the chemical equilibrium of the hydrolysis of TEOS in the reaction system.

The size and morphology of the Au@pSiO$_2$ are almost not changed, even after being annealed at 700 °C (Fig. 2), indicating the high sintering-resistant performance of the Au@pSiO$_2$. Au/SiO$_2$ was prepared for the comparing of the stability of the Au@pSiO$_2$. The TEM images of the Au/SiO$_2$ annealed at different temperatures are illustrated in Fig. S1. It can be seen that the Au NPs fail to withstand sintering even when annealed at 350 °C, and that Au/SiO$_2$ cannot be used to investigate the nature of Au, due to the changes of Au size and Au species during the calcination process.

Catalytic performance of Au@pSiO$_2$ NPs. 4-NP, as a toxic pollutant, is difficult to degrade. 4-AP is a useful raw material in medicine, chemical industry and so on. The catalytic reduction of 4-NP over Au NPs in the presence of NaBH$_4$ has been widely investigated for the production of 4-AP.[27] Therefore, we utilized the reduction of 4-NP to 4-AP with excess NaBH$_4$ as a model reaction to study catalytic activity of the Au@pSiO$_2$, and the as-prepared Au@pSiO$_2$ provides convenience for exploring the nature of Au and the influence of the surfactant on catalytic performance. The process can be monitored by UV-Vis spectrum because 4-NP and 4-AP have different absorbances in the UV-Vis range (λmax= 400 nm and 300 nm, respectively).[28]

The pale yellow aqueous solution of 4-NP was changed into dark yellow after NaBH$_4$ was added in. A red shift with absorption maximum at 400 nm was observed immediately after the adding of NaBH$_4$, which is illustrated in Fig. S2a. This is due to the formation of 4-nitrophenolate ions in a NaBH$_4$ medium.[29] Control experiments demonstrate that the reduction reaction is not catalyzed by NaBH$_4$ aqueous solution (Fig. S2b). When a trace amount of the Au@pSiO$_2$ was introduced, successive fading of the characteristic yellow colour of the 4-nitrophenolate ions was observed. Figs. 3a-3d show typical examples of such reduction catalyzed by the Au@pSiO$_2$ annealed at different temperatures, from which the conversion curves and plots of ln(C_t/C_0) against reaction time where C_t and C_0 are the concentrations of the 4-NP at times t and 0, respectively, were obtained (Figs. 3e and 3f). As can be seen from Fig. 3, the catalytic activity is enhanced after Au@pSiO$_2$ annealed at different temperatures, and the sample annealed at 500 °C has the

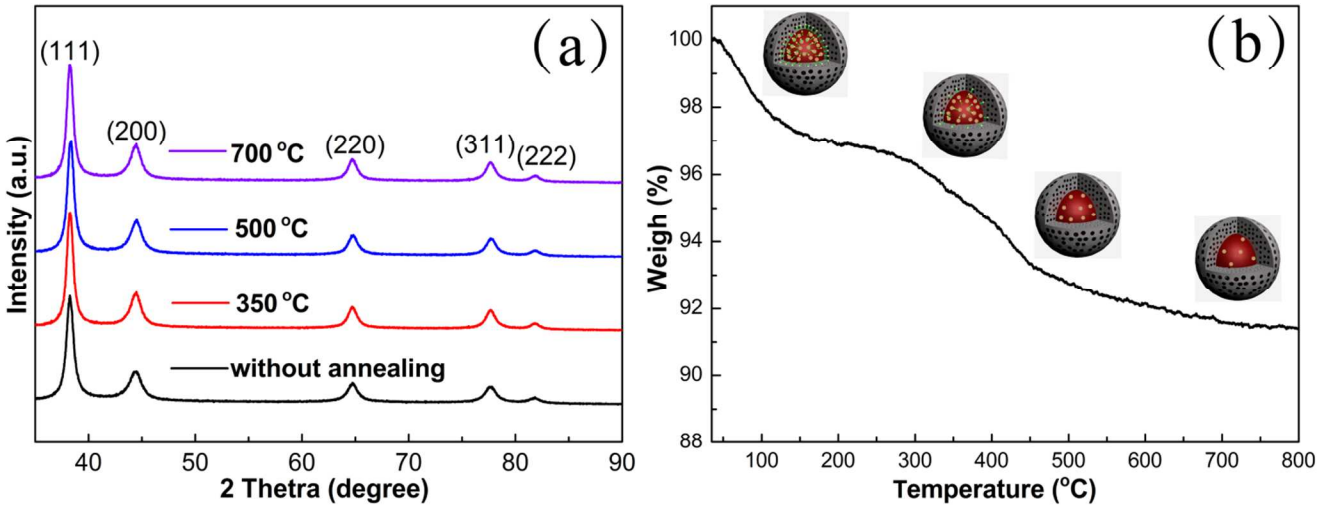

Fig. 4 (a) XRD patterns of the Au@pSiO$_2$ annealed at different temperatures, (b) TG curve of the Au@pSiO$_2$.

best performance, followed by the samples annealed at 350 °C and 700 °C. The kinetic constant k is 14*10^{-3} s^{-1} μmol Au^{-1}, which is higher than that of the other Au-containing nanocatalysts reported in the literatures (Table S1). It was reported that the activity of the sample SiO$_2$/Pt@SiO$_2$ annealed at 800 °C was below that of the untreated sample for the reduction of 4-NP, which was due to the agglomeration of Pt NPs.[30] In our work, as the size of the Au is maintained even after being annealed at 700 °C, the effect of the size of the Au on the catalytic performance is excluded. To discover the reason why the samples annealed at different temperatures show different catalytic performances, we carried out XRD analysis, TG analysis and so on. For Au@pSiO$_2$ NPs, the characteristic diffraction peaks correspond to the diffraction pattern of cubic phase Au (PDF 01-1172), and the XRD patterns (Fig. 4a) are similar to those reported in the literature.[31] There is almost no difference for XRD patterns of the four samples, indicating that crystallinity have no influence on catalytic performance.

Fig. 4b shows the TG curve of the Au@pSiO$_2$.The weight loss of the sample resulted from 20-200 °C can be ascribed to the physically and chemically absorbed water and other organic species with low molecular weights. There is a significant weight loss at temperature above 200 °C, where PVP starts decomposing. A slight decreasing in weight can be seen above 500 °C, indicating that PVP is nearly totally removed from the surfaces of the Au NPs. The FTIR spectra of the Au@pSiO$_2$ annealed at different temperatures are shown in Fig. S3. For reference, the obtaining of the spectrumof pure PVP was also conducted. The bands at 2850 cm^{-1} and 2920 cm^{-1}, which can be ascribed to the characteristic frequencies of the antisymmetric and symmetric stretching vibrations of methylene in PVP molecules, respectively, are observed in the untreated NPs and the sample annealed at 350 °C. The C-H bands disappear for the samples annealed at 500 °C and 700 °C, suggesting the nearly completely removing of PVP from the surfaces of the Au NPs annealed at 500 °C and 700 °C.

It is well known that organic molecules or other species located at the surfaces of the metal NPs have effects on the catalytic performance, which involves the exposure of active sites. From the TG curve and the IR spectra, we can find that PVP is partly and nearly fully removed at 350 °C and 500 °C, respectively. For the annealed samples, new active sites of Au NPs that are occupied by PVP beforehand are exposed, resulting in the enhanced activity. With the increase of the annealing temperature, PVP located at the surfaces of the Au NPs is decomposed and the catalytic activities increase gradually. In other words, the removal of the surfactant PVP is important for catalytic performance, which benefits from the new exposing of the active sites of the Au NPs occupied by PVP beforehand.

The relative amount of Au species can be changed during the thermal annealing process. As Au species affect the catalytic activity greatly, XPS spectra were used to further investigate the effect of Au species on the catalytic performance for the Au@pSiO$_2$. Au species were analyzed by XPS spectrum combining with XPS PEAK41 software, and four peaks centered at around 83.8, 87.5, 84.5 and 88.2 eV were obtained (Fig. 5 and Table S2). The peaks at round 83.8 and 87.5 eV can be assigned

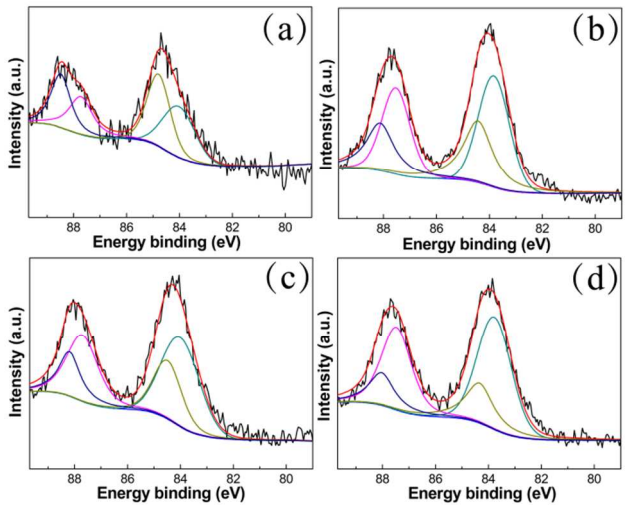

Fig. 5 Au 4f XPS spectra of Au@pSiO$_2$ annealed at different temperatures: (a) without annealing, (b) 350 °C, (c) 500 °C, and (d) 700 °C.

to Au^0, and other peaks can be assigned to Au^{n+} according to the reports in the literatures.[32-38] The XPS results reveal that the relative intensity of Au^{n+} declines steadily when increasing the annealing temperature, which is consistent with that reported in the literatures.[39-41] when the annealing temperatures are 500 and 700 °C, PVP is nearly completely removed from the surfaces of the samples. The Au^{n+}/Au^0 ratio of the samples annealed at 500 and 700 °C are 0.56 and 0.41, respectively. The catalytic activity of the Au@pSiO_2 annealed at 700 °C is lower than that of the Au@pSiO_2 annealed at 500 °C due to the lower content of cationic Au, which indicates that cationic Au species play a vital role in the reduction of 4-NP.

The relative intensity of Au^{n+} for the sample annealed at 350 °C is higher than that for the sample annealed at 500 °C, but a portion of PVP is still located at the surfaces of the Au NPs for the sample annealed at 350 °C, leading to similar activities for the two samples. Although the ratio of Au^{n+}/Au^0 of the untreated sample is higher than those of the annealed samples, the surfactant PVP located at the surface of the Au for the untreated sample results in the lower activity. In brief, not only PVP but also the cationic Au species have effects on catalytic performance for the reduction of 4-NP. These results will be beneficial to surface cleaning and pretreatment condition determining of catalysts, especially Au-based catalysts.

Induction period. Interestingly, it is also found that an induction period existed during the reduction process of the untreated Au@pSiO_2 (Fig. 3, black curve). That is, the concentration of 4-NP changes slowly initially, and become fast suddenly after a specific reaction time, and then decreases step by step. Induction period disappeared for the annealed samples. It was reported that the induction period was attributed to the diffusion of reactants into the inner spaces resulting from pore structure.[42] However, Zhang's group[43] reported that the induction period was dependent on the size of the Au core encapsulated in the Au@mSiO_2 yolk-shell NPs, and the induction period disappeared when the size of the Au core was smaller than 21 nm. Camargo's group[44] prepared Au/TiO_2 NPs and found that the induction period was also dependent on the size of the Au NPs. Because of the direct exposing of the Au NPs to the reactants, there was no diffusion process. Therefore, the induction period cannot be only ascribed to the resistance resulting from diffusion. In this work, the induction period disappeared for the annealed Au@pSiO_2 while the pore structure remained. Thus, the diffusion of the reactants resulting from pore structure of the Au@pSiO_2, which leads to the induction period, was implausible.

In general, induction period is a process of regulating the activity of the surface conditions of catalysts under catalytic reaction system. It is the synergism effect between the property changes of the catalyst surface and the adsorption or migration of catalytic substrate. $NaBH_4$, as a strong reductant, may alter the surface conditions of catalysts, which probably results in the induction period. After the Au@pSiO_2 had been soaked in $NaBH_4$ solution for 15 min, the reduction reaction was initiated when 4-NP was added in. It is clearly seen that the induction period still exists (as shown in Fig. S4), which indicates that the $NaBH_4$ cannot activate the Au@pSiO_2, and the induction period cannot be induced by $NaBH_4$. Moreover, we also carried out the

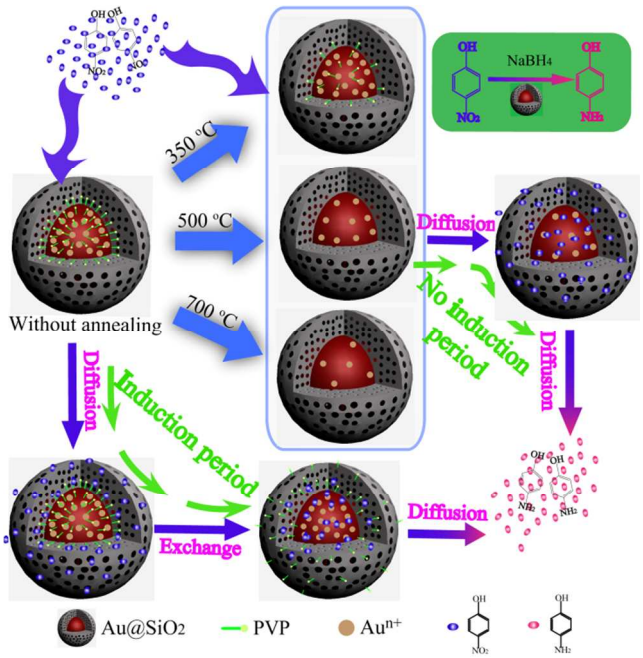

Scheme 2 Schematic illustration of catalysis mechanism for Au@pSiO_2 annealed at different temperatures.

experiment to verify whether 4-NP can activate Au. The result is also illustrated in Fig. S4 and the induction period still exists, indicating that 4-NP cannot activate the Au@pSiO_2. Normally, structure determines properties. The distinct difference was the removal of PVP between the annealed Au@pSiO_2 and the untreated Au@pSiO_2. Because of the competition between 4-nitrophenol and PVP on the surfaces of Au NPs, PVP blocks the adsorption and migration of 4-NP on the surfaces of the Au NPs, leading to the appearing of the induction period for the untreated Au@pSiO_2. When PVP was removed, 4-NP can be easily diffused and migrated on the surface of the Au, resulting in the disappearing of the induction period for the annealed Au@pSiO_2. In other words, PVP is the key factor to the induction period.

Catalysis mechanism for Au@pSiO_2 NPs. Based on the above results, the catalysis mechanism can be summarized, as shown in Scheme 2. PVP is used for stabilizing Au in the synthetic process and exists between the Au core and the SiO_2 shell in the Au@pSiO_2. PVP is removed gradually from the surfaces of the Au NPs with the increase of the annealing temperature, leading to the enhancing of the activity of the Au@pSiO_2. However, the cationic Au species decrease gradually with the increase of the annealing temperature, resulting in the lower activity of the Au@pSiO_2 annealed at 700 °C than that of the Au@pSiO_2 annealed at 500 °C at the same time when PVP is removed completely. Thanks to the combined effect of Au species and the surfactant PVP on activity, the sample annealed at 500 °C has a performance similar to the sample annealed at 350 °C.

There is competition between 4-NP and PVP on the surfaces of the Au NPs. When the untreated Au@pSiO_2 is added to the 4-NP and $NaBH_4$ solution, 4-NP diffuses into the interior of the Au@pSiO_2, and PVP blocks the absorption and migration of 4-NP on the surfaces of the Au NPs, resulting in the appearing of the induction period. For the annealed Au@pSiO_2, PVP is removed and 4-NP can be easily absorbed onto the surfaces of the

Au NPs. Therefore, the induction period disappears. Although a portion of PVP is remained in the Au@$pSiO_2$ annealed at 350 °C, the amount of PVP is too little to block 4-NP, also leading to the disappearing of the induction period.

Conclusions

In summary, the Au@$pSiO_2$ was prepared by using typical Stober method combined with hydrothermal etching, and the effects of Au species and PVP on the catalytic activity of 4-nitrophenol reduction in thermal annealing process were investigated. The activity of the Au@$pSiO_2$ was enhanced after annealing because of the removal of PVP, and the Au@$pSiO_2$ annealed at 500 °C had the best performance. The removal of the surfactant was necessary to obtain highly active catalysts. However, the annealing temperature should not be too high because of the decrease of cationic Au species, which was important in catalyzing the reduction of 4-NP. That is, the cationic Au species and the surfactant PVP had a combined effect on catalytic performance. We believe that these results will be beneficial to improve catalytic activity, and develop advanced Au-based catalysts.

Acknowledgement

This work was supported by the China National Natural Science Fund (Nos.21275016).

Notes and references

*State Key Laboratory of Chemical Resource Engineering, BeijingUniversity of Chemical Technology, Beijing 100029, China. *E-mail:gufb@mail.buct.edu.cn*

†Electronic Supplementary Information (ESI) available: TEM, UV-Vis spectra, IR results, and XPS data are included. See DOI: 10.1039/b000000x/

1 Q. Ji, J. Hill and K. Ariga, *J. Mater. Chem. A*, 2013, **1**, 3600.
2 L. He, Y. Liu, J. Liu, Y. Xiong, J. Zheng, Y. Liu and Z. Tang, *Angew. Chem. Int. Ed.*, 2013, **52**, 3741.
3 G. Li and R. Jin, *Acc. Chem. Res.*, 2013, **46**, 1749.
4 P. Li, Z. Wei, T. Wu, Q. Peng and Y. Li, *J. Am. Chem. Soc.*, 2011, **133**, 5660.
5 C. Chiu, P. Chung, K. Lao, C. Liao and M. Huang, *J. Phys. Chem. C*, 2012, **116**, 23757.
6 M. Langille, M. Personick, J. Zhang and C. Mirkin, *J. Am. Chem. Soc.*, 2012, **134**, 14542.
7 P. Chung, L. Lyu and M. Huang, *Chem. Eur. J.*, 2011, **17**, 9746.
8 N. Naresh, F. Wasim, B. Ladewig and M. Neergat, *J. Mater. Chem. A*, 2013, **1**, 8553.
9 M. Crespo-Quesada, J. Andanson, A. Yarulin, B. Lim, Y. Xia and L. Kiwi-Minsker, *Langmuir*, 2011, **27**, 7909.
10 D. Li, C. Wang, D. Tripkovic, S. Sun, N. Markovic and V. Stamenkovic, *ACS Catal.*, 2012, **2**, 1358.
11 G. Hutchings, M. Hall, A. Carley, P. Landon, B. Solsona, C. Kiely, A. Herzing, M. Makkee, J. Moulijn, A.Overweg, J. Fierro-Gonzalez, J. Guzman and B. Gates, *J. Catal.*, 2006, **242**, 71.
12 J. Fierro-Gonzalez and B. Gates, *Catal. Today*, 2007, **122**, 201.
13 J. Guzman and B. Gates, *J. Am. Chem. Soc.*, 2004, **126**, 2672.
14 X. Zhang, H. Shi and B. Xu, *J. Catal.*, 2011, **279**, 75.
15 W. Wang, L. Lyu and M. Huang, *Chem. Mater.*, 2011, **23**, 2677.
16 C. Kuo, T. Hua and M. Huang, *J. Am. Chem. Soc.*, 2009, **131**, 17871.
17 L. Kong, W. Chen, D. Ma, Y. Yang, S. Liu and S Huang, *J. Mater. Chem.*, 2012, **22**, 719.
18 J. Du, J. Qi, D. Wang and Z. Tang, *Energy Environ. Sci.*, 2012, **5**, 6914.
19 T. Butburee, Y. Bai, J. Pan, X. Zong, C. Sun, G. Liu and L. Wang, *J. Mater. Chem. A*, 2014, **2**, 12776.
20 M. Cargnello, J. Jaén, J. Garrido, K. Bakhmutsky, T. Montini, J. Gámez, R. Gorte and P. Fornasiero, *Science*, 2012, **37**, 713.
21 W. Shi, H. Zeng, Y. Sahoo, T. Ohulchanskyy, Y. Ding, Z. Wang, M. Swihart and P. Prasad, *Nano Lett.*, 2006, **6**, 875.
22 Z. Bao, Z. Sun, Z. Li, L. Tian, T. Ngai and J. Wang, *Langmuir*, 2011, **27**, 5071.
23 N. Yan, Q. Chen, F. Wang, Y. Wang, H. Zhong and L. Hu, *J. Mater. Chem. A*, 2013, **1**, 637.
24 A. Guerrero-Martınez, J. Perez-Juste and L. Liz-Marzan, *Adv. Mater.*, 2010, **22**, 1182.
25 Y. Chen, H. Chen, L. Guo, Q. He, F. Chen, J. Zhou, J. Feng and J. Shi, *ACS Nano*, 2010, **4**, 529.
26 Y. Wong, L. Zhu, W. Teo, Y. Tan, Y. Yang, C. Wang and H. Chen, *J. Am. Chem. Soc.*, 2011, **133**, 11422.
27 J. Zeng, Q. Zhang, J. Chen and Y. Xia, *Nano Lett.*, 2010, **10**, 30.
28 Y. Qiu, Z. Ma and P. Hu, *J. Mater. Chem. A*, 2014, **2**, 13471.
29 P. Dauthal and M. Mukhopadhyay, *Ind. Eng. Chem. Res.*, 2012, **51**, 13014.
30 P. Lu, C. Campbell and Y. Xia, *Nano Lett.*, 2013, **13**, 4957.
31 X. Zhang, Y. Zhu, X. Yang, Y. Zhou, Y. Yao and C. Li, *Nanoscale*, 2014, **6**, 5971.
32 D. Bulushev, I. Yuranov, E. Suvorova, P. Buffat and L. Kiwi-Minsker, *J. Catal.*, 2004, **224**, 8.
33 Y. Liu, H. Dai, J. Deng, L. Zhang, B. Gao, Y. Wang, X. Li, S. Xie and G. Guo, *Appl. Catal. B*, 2013, **140–141**, 317.
34 S. Xie, H. Dai, J. Deng, Y. Liu, H. Yang, Y. Jiang, W. Tan, A. Ao and G. Guo, *Nanoscale*, 2013, **5**, 11207.
35 S. Xie, H. Dai, J. Deng, H. Yang, W. Han, H. Arandiyan and G. Guo, *J. Hazard. Mater.,* 2014, **279**, 392.
36 X. Liu, M. Liu, Y. Luo, C. Mou, S. Lin, H. Cheng, J. Chen, J. Lee and T. Lin, *J. Am. Chem. Soc.*, 2012, **134**, 10251.
37 X. Li, H. Dai, J. Deng, Y. Liu, S. Xie, Z. Zhao, Y. Wang, G. Guo and H. Arandiyan, *Chem. Eng. J.*, 2013, **228**, 965.
38 S. Minicò, S. Scirè, C. Crisafulli and S. Galvagno**,** *Appl. Catal. B*, 2001, **34**, 277.
39 X. Zhang, H. Shi and B. Xu, *Catal. Today*, 2007, **122**, 330.
40 Q. Ye, J. Zhao, F. Huo, D. Wang, S. Cheng, T. Kang and H. Dai, *Micropor. Mesopor. Mat.*, 2013, **172**, 20.
41 X. Zhang, H. Shi and B. Xu, *Angew. Chem. Int. Ed.*, 2005, **44**, 7132.
42 B. Liu, S. Yu, Q. Wang, W. Hu, P. Jing, Y. Liu, W. Jia, Y. Liu, L. Liu and J. Zhang, *Chem. Commun.*, 2013, **49**, 3757.
43 S. Wang, M. Zhang and W. Zhang, *ACS Catal.*, 2011, **1**, 207.

44 T. Damato, C. Oliveira, R. Ando and P. Camargo, *Langmuir*, 2013, **29**, 1642.

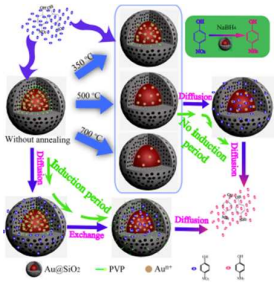

The cationic Au species and surfactant of the Au@pSiO$_2$ had a combined effect on the catalytic reduction of 4-NP.